

## Around the Spindle galaxy: the dark halo mass of NGC3115.

I. D. KARACHENTSEV,<sup>1</sup> L. N. MAKAROVA,<sup>1</sup> G. S. ANAND,<sup>2</sup> AND R. B. TULLY<sup>3</sup>

<sup>1</sup>*Special Astrophysical Observatory, the Russian Academy of Sciences, Nizhnij Arkhyz, KChR, 369167, Russia*

<sup>2</sup>*Space Telescope Science Institute, 3700 San Martin Drive, Baltimore, MD 21218, USA*

<sup>3</sup>*Institute for Astronomy, University of Hawaii, 2680 Woodlawn Drive, Honolulu, HI 96822, USA*

### ABSTRACT

We report observations of five dwarf galaxies in the vicinity of the luminous S0 galaxy NGC 3115 performed with the Advanced Camera for Surveys on the Hubble Space Telescope. Their distances determined via the Tip of the Red Giant Branch are: 10.05 Mpc (UGCA 193), 9.95 Mpc (KKSG 17), 10.13 Mpc (2MASX-J0957-0915), 10.42 Mpc (2dFGRS-TGN218Z179) and 11.01 Mpc (KKSG 19). With their typical distance error of about 0.75 Mpc all the five dwarfs are consistent to be true satellites of the host galaxy NGC 3115 ( $10.2 \pm 0.2$  Mpc). Using the DESI Legacy Imaging Surveys we also found 5 new probable dwarf satellites of NGC 3115, as well as 4 new probable members of the neighboring group around NGC 3521 situated 3 Mpc away from the NGC 3115 group. Based on the radial velocities and projected separations of 10 dwarf companions, we derived the total (orbital) mass of NGC 3115 to be  $(4.89 \pm 1.48) 10^{12} M_{\odot}$ . The ratio of the total mass-to-K-luminosity of NGC 3115 is  $(50 \pm 15) M_{\odot}/L_{\odot}$ , which is typical for the early-type luminous galaxies.

*Keywords:* galaxies: distances and redshifts - galaxies: dwarf

### 1. INTRODUCTION.

According to modern concepts, the bulk of the matter of galaxies is contained in their dark halos, the nature of which remains unclear. The fundamental parameter of a galaxy is the ratio between its

total mass,  $M_T$ , and stellar mass,  $M_*$ . The dimensionless quantity  $M_T/M_*$  characterizes the history of star formation in the galaxy, as well as its present dynamic status. In recent years, many publications have appeared in which the magnitude of  $M_T/M_*$  is modeled depending on the luminosity or mass of the galaxy (Sales et al. 2013; Moster et al. 2013; Wechsler & Tinker 2018; Santos-Santos et al. 2021). As shown by theoretical calculations and observational results, the minimum ratio  $M_T/M_*$  occurs for galaxies of the Milky Way type with  $M_*/M_\odot \sim 11$  dex, increasing both towards more massive galaxies and towards dwarf systems (Kourkchi & Tully 2017; Lapi et al. 2018; Posti & Fall 2021).

In addition to the dependence on the mass (luminosity) of a galaxy, the ratio  $M_T/M_*$  also depends on its morphological type. Spiral galaxies of type Milky Way and M 31 have an  $M_T/M_* \sim 25$ , while early-type galaxies (ETG) with dominant bulges are characterized by an  $M_T/M_*$  ratio that is 2–3 times higher (Karachentseva et al. 2011; Mandelbaum et al. 2016; Bilicki et al. 2021). This difference may be due to the fact that star formation in disk-dominated galaxies occurs fairly evenly throughout the entire cosmological scale of 13.8 Gyr, while the main (violent) formation of stars in E and S0 galaxies ended in an early epoch, almost ceasing in the last 10 Gyr. At the same time, early-type galaxies are not inferior to late-type galaxies in terms of integral luminosity and stellar mass. For example, in the Local Volume, limited by the distance  $D < 11$  Mpc, the five brightest relatively isolated galaxies of the S0 type (NGC 4594, NGC 3115, NGC 1291, NGC 5128 and NGC 2784) have an average K-band luminosity  $\langle \log(L_K/L_\odot) \rangle = 10.99 \pm 0.09$ , while the five brightest spiral galaxies of the Sc-Scd type (NGC 6946, NGC 253, NGC 5194, NGC 5236 and M 101) have an average luminosity of  $\langle \log(L_K/L_\odot) \rangle = 10.92 \pm 0.04$  (Karachentsev & Kashibadze 2021). Obviously, the  $M_T/M_*$  ratio in galaxies is influenced not only by the history of star formation in them, but also by the repeated process of merging of the galaxy with its surrounding neighbors. Being in a denser environment, E and S0 galaxies are likely to experience more frequent mergers and, therefore, turn out to be among the leaders in terms of integral luminosity. The total (dynamic) mass of E and S0 galaxies is usually determined from the dispersion of the line-of-sight velocities of stars, globular clusters or planetary nebulae (Capaccioli et al. 1993; Peng et al. 2004; Guerou et al. 2016; Bilek et al. 2019). These

estimates correspond to a linear scale of  $\sim(20\text{--}50)$  kpc and obviously underestimate the total mass of the galaxy within the virial radius of its halo,  $R_{vir} \sim 350$  kpc. To determine  $M_T$  for isolated E and S0 galaxies, data on radial velocities and projected separations of small satellites of these galaxies are most suitable. Of particular interest here are the ETG galaxies of the Local Volume, where the observational data on accurate distances and velocities of galaxies are most complete in comparison with distant volumes. At present, fairly reliable estimates of the total mass have been made for only two ETG galaxies of the Local Volume: NGC 5128 (Centaurus A) and NGC 4594 (Sombrero) (Karachentsev et al. 2020; Karachentsev & Kashibadze 2021). In this article, we measure the distances to 5 satellites of the S0 galaxy NGC 3115 (Spindle galaxy) and determine the total mass of this host galaxy.

In section 2, we present images of 5 dwarf galaxies in the vicinity of NGC 3115, obtained with the Hubble Space Telescope (HST), and estimate the distances of these galaxies via the Tip of Red Giant Branch (TRGB) in color-magnitude diagrams (CMD). In section 3, we report on the detection of five new candidates for satellites of NGC 3115 and give a summary of the parameters of 27 putative satellites of NGC 3115, whose radial velocities and projected separations determine the orbital (total) mass of the central galaxy,  $M_T$ . Section 4 is devoted to the group of dwarf satellites around the Sbc galaxy NGC 3521, adjacent to the group around NGC 3115. The dark halo of galaxy NGC 3521 is distinguished by an abnormally low  $M_T/M_*$  ratio. Section 5 presents a summary of mass estimates for 5 isolated high-luminosity ETC-galaxies in the Local Volume. Our conclusions are summarized in section 6.

## 2. HST OBSERVATIONS AND NEW TRGB DISTANCES.

One hundred and fifty target galaxies were selected by us for observations with the ACS camera on the HST within the SNAP-15922 program "Every Known Nearby Galaxy" (PI R.B. Tully). Of these, 80 galaxies, mainly dwarf systems, were observed in the filters F606W and F814W with exposures of 760 sec in each filter during 2019-2020. The five observed galaxies are located in the vicinity of the bright ( $B = 9.9$  mag) lenticular galaxy NGC 3115, which has a heliocentric radial velocity  $V_h = (681 \pm 6)$  km s $^{-1}$  (Wegner et al. 2003). The distance to it,  $D = (9.68 \pm 0.40)$  Mpc,

was determined by Tonry et al. (2001) via surface brightness fluctuations (SBF). Later Peacock et al (2015) specified its distance,  $D = (10.2 \pm 0.2)$  Mpc, using the TRGB method. One of the NGC 3115 neighbors we observed, UGCA 193 = PGC 029086, is a spiral Sd galaxy seen edge-on. Its angular Holmberg diameter, 4.3 arcmin, exceeds the size of the ASC field-of-view. The remaining 4 objects: KKSG 17=MCG-01-26-011=PGC 029033, 2MASX-J09570887-0915487=PGC 154449, 2dFGRS-TGN218Z179=PGC 1099440 and KKSG 19= PGC 3097700 are irregular (dIrr) or blue compact dwarf (BCD) galaxies with angular sizes of 0.7 - 0.9 arcmin. Their ACS images, created with the F606W (blue), F814W (red), and the average of the two images (green) are shown in the Figure 1.

The obtained images were processed by the standard HST pipeline (Dolphin 2000, 2016) with the recommended DOLPHOT parameters:  $(Crowd_{F606W} + Crowd_{F814W}) < 0.8$  and  $(Sharp_{F606W} + Sharp_{F814W})^2 < 0.075$ . Stars with a signal-to-noise ratio  $S/N \geq 3$  in F606W and  $S/N \geq 4$  in F814W filter were selected. Since each of the 5 galaxies occupied a small area of the ACS field of view, we excluded from the analysis objects located far beyond the optical boundaries of galaxies. In case of UGCA 193, we also excluded objects in the central part of the galactic disk with extremely high stellar density.

The resulting CMDs in F606W-F814W vs. F814W are presented in five panels of Figure 2. The diagrams show the stars of the young and old populations of galaxies. The position of the Tip of the Red Giant Branch was determined by the discontinuity on the luminosity function of stars within the colors  $[0.5 < F606W - F814W < 1.5]$  in a maximum likelihood analysis described by Makarov et al. (2006) and updated by Wu et al. (2014). In this method, the luminosity functions of the Red Giant Branch stars and Asymptotic Giant Branch populations are fitted by a broken power law, with the break signifying the location of the TRGB. The TRGB positions are marked on the CMDs with horizontal lines. Artificial stars were created and recovered using the same DOLPHOT parameters to estimate the photometric errors. The results are given in Table 1, where  $F814W_{TRGB}$  means the position of the TRGB,  $A_{814}$  - interstellar extinction in the F814W filter according to Schlafly & Finkbeiner (2011),  $M_{TRGB}$  — the zero-point calibration of the absolute magnitude of the TRGB

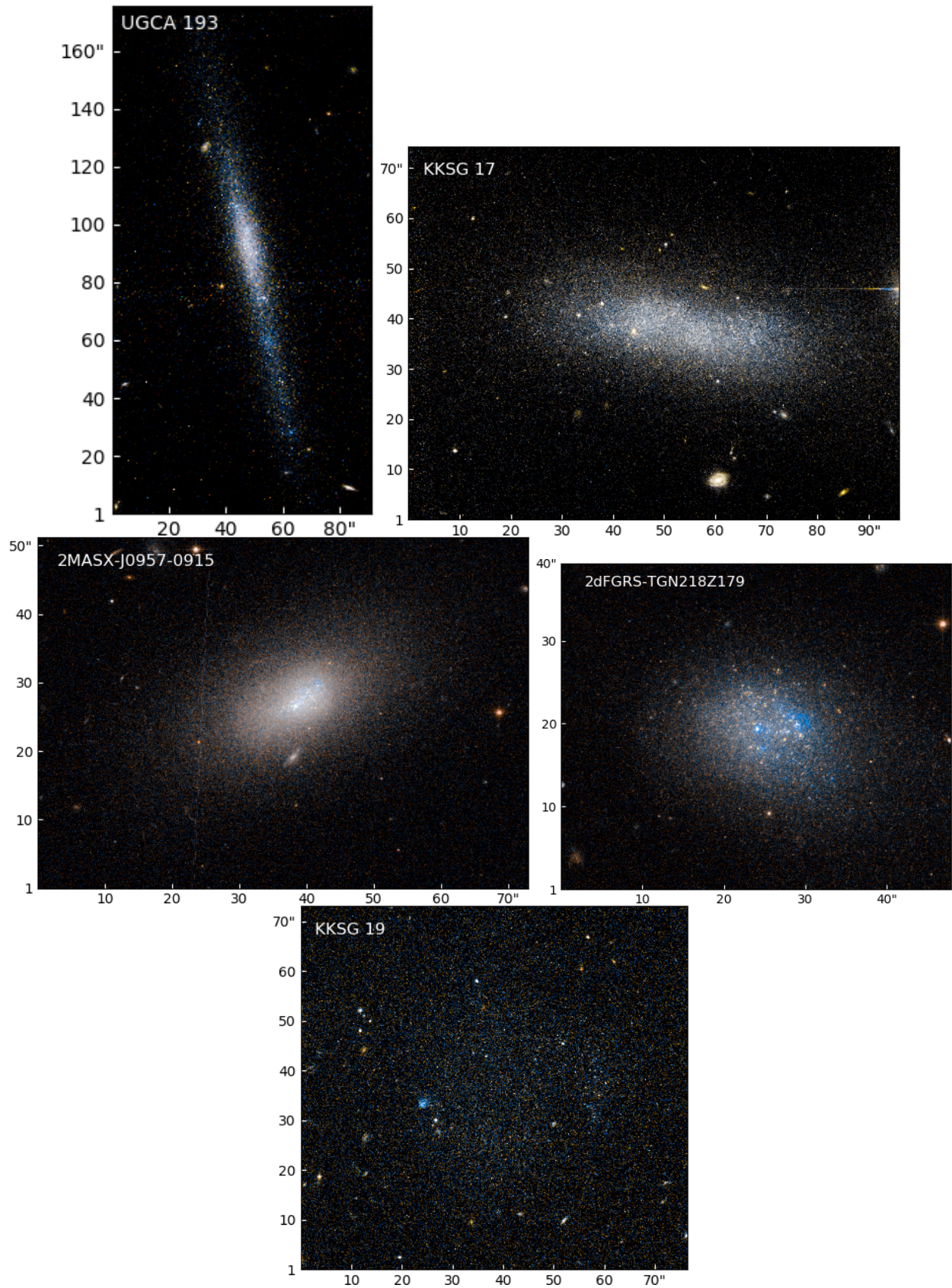


**Figure 1.** Two-color HST/ACS images of five dwarf galaxies around NGC 3115: UGCA 193, KKSG 17, 2MASX-J0957-0915, 2dFGRS-TGN218Z179 and KKSG 19. North is up and east is left.

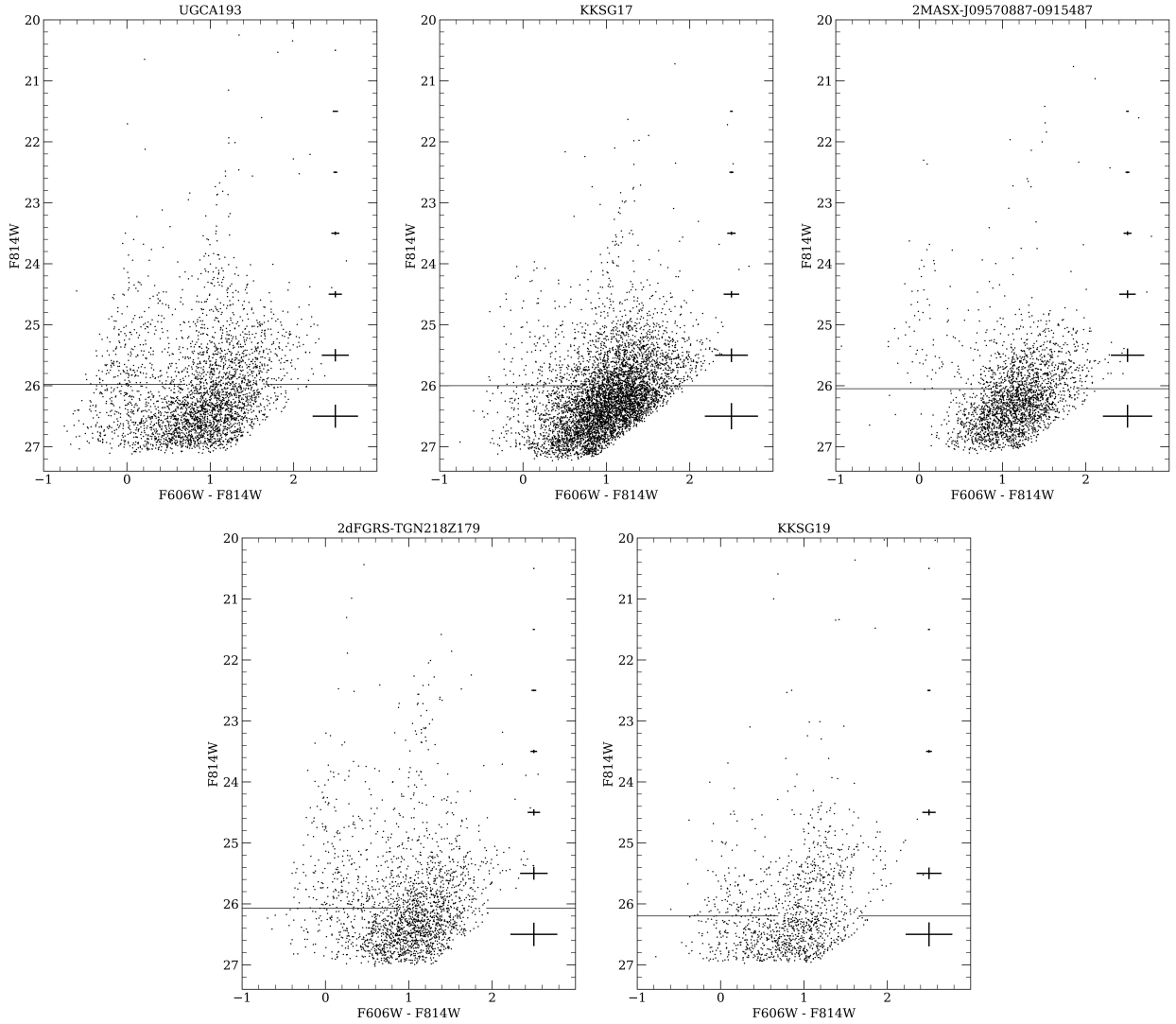


**Figure 2.** Color-magnitude diagrams of the observed galaxies. The TRGB positions are indicated by the horizontal lines. Photometric errors are shown by the bars at the right in the CMDs.

following Rizzi et al. (2007), DM and D are the distance modulus (mag) and the distance (Mpc). The typical error in determining the TRGB is about 0.15 mag, which corresponds to an error in the distance of  $\sim 0.75$  Mpc. (Some doubts, however, remain about KKSG 19, whose TRGB position is close to the CMD photometric limit). Within this error, all distances of the dwarf galaxies are in excellent agreement with the distance of the central galaxy itself ( $10.2 \pm 0.2$  Mpc). This gives reason to consider them as physical satellites of the lenticular galaxy NGC 3115.

### 3. RETINUE OF THE SPINDLE GALAXY.

**Table 1.** TRGB properties of the dwarf companions of NGC 3115.

Galaxy	$F814W_{\text{TRGB}}$	$A_{814}$	$M_{\text{TRGB}}$	$DM$	$D$
	mag	mag	mag	mag	Mpc
(1)	(2)	(3)	(4)	(5)	(6)
UGCA 193	25.98	0.060	-4.09	30.01	10.05
KKSG 17	26.00	0.090	-4.08	29.99	9.95
2MASX-J0957-0915	26.05	0.102	-4.08	30.03	10.13
2dFGRS-TGN218Z179	26.07	0.066	-4.09	30.09	10.42
KKSG 19	26.20	0.104	-4.11	30.21	11.01

Examining the SERC EJ zone of the Palomar Sky Survey, Karachentsev et al. (2000) found six low surface brightness dwarf galaxies in the vicinity of NGC 3115. Some of them were noted earlier in the MCG catalog (Vorontsov-Veliaminov & Arkhipova, 1963). Observations in the 21 cm HI line (Huchtmeier et al. 2001) showed that the radial velocities of these objects are close to the radial velocity of NGC 3115. Surveys of redshifts of southern galaxies: 2dF (Colles et al. 2003), HIPASS (Doyle et al. 2005) and 6dF (Jones et al. 2009) have added 5 more dwarf galaxies to the supposed satellites of NGC 3115. Using the DESI Legacy Imaging Surveys = DECaLS (Dey et al. 2019), Carlsten et al. (2021a) found 11 more probable dwarf satellites of NGC 3115. Their search area in this digital survey of the northern sky covered only part of the virial zone around NGC 3115. Therefore, we repeated the search for faint satellites of NGC 3115, expanding the search area to 20 square degrees. As a result, we found all 11 dwarf systems noted by Carlsten et al. (2021a), and on top of that found 5 more candidates for faint satellites of the Spindle galaxy. Color images of these galaxies taken from the DECaLS survey (Dey et al. 2019) are shown in Fig.3. The images size is 2'x2', north is up and east is left. Table 2 contains: equatorial coordinates of the galaxies, their major angular diameter in arcmin, axial ratio, morphological type, and apparent B- magnitude estimated by eye from a comparison of the new putative satellites with other dwarfs, whose g- and r- magnitudes were measured by Carlsten et al. (2021b). According to our estimates, the error in determining the visual B- magnitudes is about 0.25 mag.



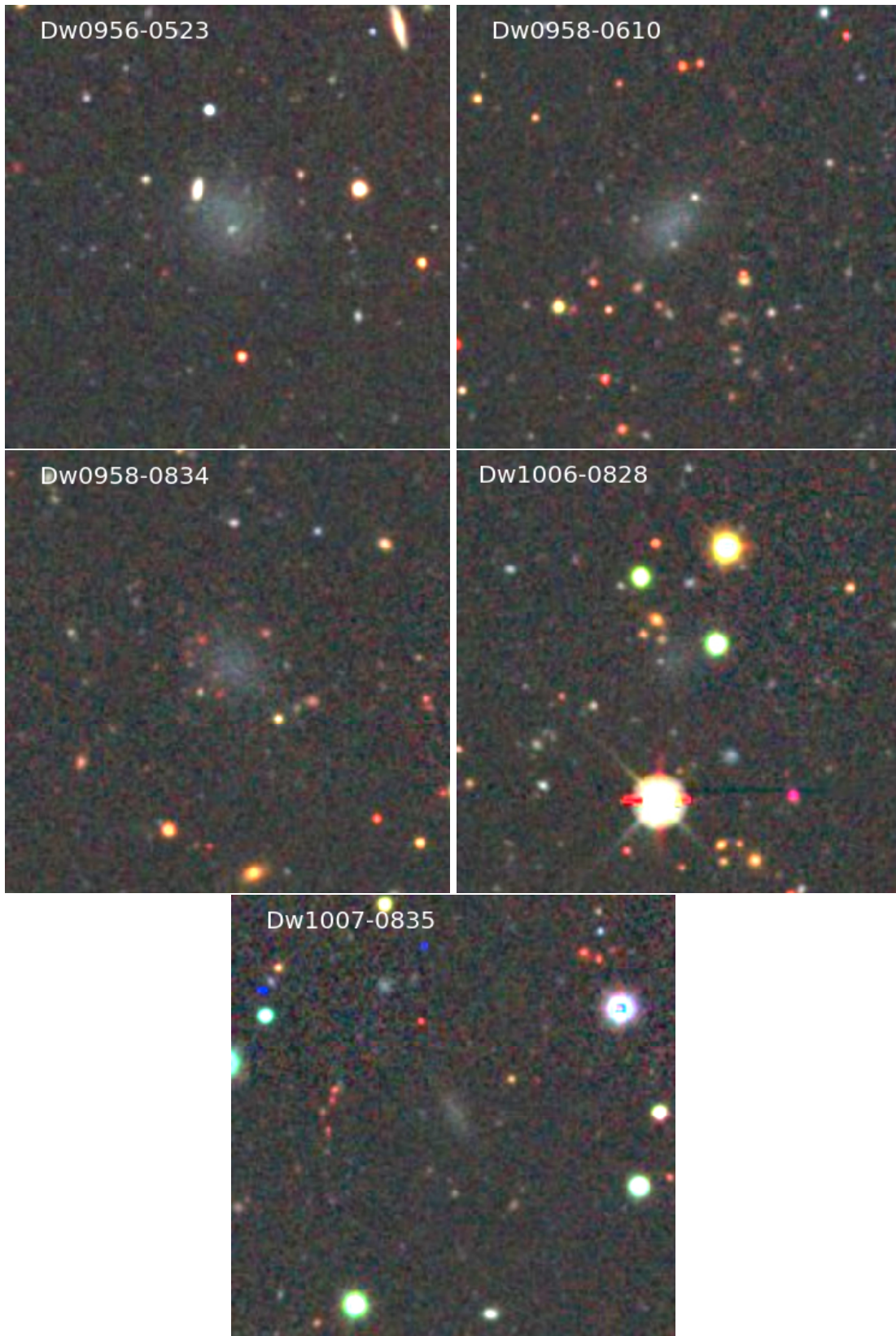


**Figure 3.** Color-composed images of five new probable satellites of NGC 3115 taken from the DECaLS survey. The size of the stamps is 2 arcminutes. North is up and east is left.



**Table 2.** New probable satellites of NGC 3115.

Name	RA (J2000.0)	DEC	$a'$	b/a	T	B
(1)	(2)	(3)	(4)	(5)	(6)	(6)
Dw0956-0523	09 56 55.6	-05 23 32	0.38	0.95	dSph	19.3
Dw0958-0834	09 58 05.5	-08 34 36	0.37	0.73	dSph	19.6
Dw0958-0610	09 58 35.3	-06 09 58	0.38	0.81	dSph	19.5
Dw1006-0828	10 06 35.8	-08 27 56	0.16	0.80	dIrr	21.6
Dw1007-0835	10 07 15.4	-08 35 11	0.30	0.33	dTr	20.3

The final summary of the 27 probable satellites of the Spindle galaxy is presented in Table 3. Its columns contain: (1) galaxy name (name in *italic* for the galaxies observed by us with HST/ACS); (2) equatorial coordinates in degrees; (3) morphological type in de Vaucouleurs scale; (4) distance to the galaxy; (5) method by which the distance is estimated: TRGB — via the luminosity of the Tip of the Red Giant Branch, SBF — via fluctuation of surface brightness, TF — from Tully-Fisher relation, NAM — by the radial velocity of galaxy in the model of Numerical Action Method (Shaya et al. 2017), mem — by implied membership in the group; (6) radial velocity of the galaxy relative to the Local Group centroid taken from NASA Extragalactic Database (=NED, <http://ned.ipac.caltech.edu/>); (7) integral luminosity of the galaxy in K-band from Updated Nearby Galaxy Catalog (= UNGC, <http://www.sao.ru/lv/lvgdb>) or from Carlsten et al. (2021a); (8) angular separation of the satellite from NGC 3115; (9) linear projected separation of the satellite under the assumption that it is at the same distance as the host galaxy; (10) the radial velocity difference between the satellite and the central galaxy; (11) orbital mass estimate of the total mass of NGC 3115 defined below. At the end of the Table, under the line, there are 4 galaxies with radial velocities close to that of NGC 3115, but which are outside the "zero-velocity radius"  $R_0 \simeq 1.3$  Mpc for the NGC 3115 group. The galaxies are ranked by angular distance from NGC 3115.

Distribution of 27 supposed satellites of the Spindle galaxy is presented in Fig.4 in equatorial coordinates. The galaxies of early types ( $T < 0$ ) and late types ( $T > 0$ ) are indicated by red and blue symbols, respectively. The size of the circles is proportional to the logarithm of the galaxy's

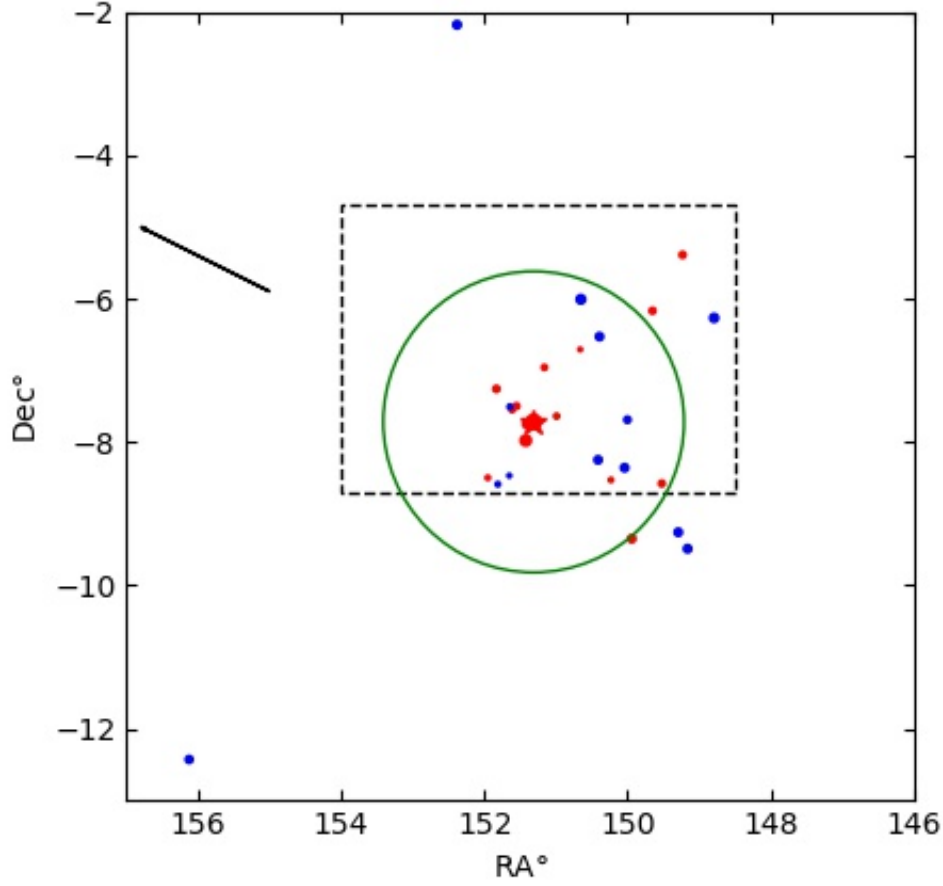


**Figure 4.** The distribution of companions around the Spindle galaxy (NGC 3115) in equatorial coordinates. The early-type galaxies and late-type galaxies are indicated by red and blue symbols, respectively. The green ring corresponds to the virial radius of 365 kpc around the NGC 3115. The rectangular perimeter delineates our viewing area on the DESI Legacy Imaging Surveys. The arrow marks the direction towards the neighboring group around NGC 3521.

K-luminosity. The virial region with a radius  $R_{vir} = 365 \text{ kpc} = 2.05 \text{ deg}$ , corresponding to the virial mass of  $4.910^{12} M_{\odot}$  (see below), is outlined by a green ring. The dotted rectangle shows the area of our view. Its southern perimeter is conditioned by the existing border of Legacy survey. The arrow points towards nearby bright galaxy NGC 3521. The panorama of dwarf retinue around NGC 3115 reveals several features:

- Almost half of the virial zone to the north-east of NGC 3115 is free of dwarf satellites down to the absolute magnitude  $M_B = -10$  mag. The reason for this asymmetry can be caused by the presence in this group of two flat (or linear) structures, to which the dwarf members are concentrated. This effect takes place in the Local Group and in other neighboring groups (Pawlowski et al. 2013; Ibata et al. 2014; Libeskind et al. 2015; Mueller et al. 2018).
- Distribution of the assumed satellites shows a tendency to group them into multiple subsystems at a scale of about 50 kpc. An example of such crowding in the Local Group is the pair of dwarfs NGC 147 and NGC 185. Radial velocity measurements of members of these substructures could clarify whether they are physically binded systems or due to a random projection effect.
- The distribution of dwarf galaxies along the radius of the group shows signs of morphological segregation: dSphs are more common near the host galaxy than dIrrs. This is the well-known effect seen in the Local Group and other nearby groups (Mateo, 1998 and references therein). However, there are several dSphs at a projected separation of 300–500 kpc, which indirectly indicates a significant extent of dark halo of Spindle galaxy.

The average projected separation of the 27 supposed satellites is  $\langle R_p \rangle = 302 \pm 53$  kpc, and the rms difference in radial velocities of 10 satellites relative to NGC 3115 is  $\langle \Delta V^2 \rangle^{1/2} = 105$  km s<sup>-1</sup>. Following Karachentsev & Kudrya (2014), we determined the orbital mass of the host Spindle galaxy as

$$M_T = (16/\pi)G^{-1}\langle \Delta V^2 R_p \rangle,$$

where  $G$  is the gravitation constant. It is assumed here that the faint satellites of the central galaxy move along arbitrarily oriented Keplerian orbits with an average orbital eccentricity  $e \simeq 0.7$ . Individual estimates of  $M_T$  for each satellite with measured radial velocity are indicated in the last column of Table 3. The average orbital estimate of the total mass of NGC 3115 is  $(4.89 \pm 1.48)10^{12}M_\odot$ , and the average ratio of the total mass to the luminosity is  $M_T/L_K = (50.0 \pm 15.1)M_\odot/L_\odot$ , which

is almost two times higher than the analogous ratio for the Milky Way,  $(23 \pm 8)M_{\odot}/L_{\odot}$ , and M 31,  $(31 \pm 6)M_{\odot}/L_{\odot}$  (Karachentsev & Kashibadze 2021).

#### 4. A NEIGHBORING GROUP OF GALAXIES AROUND NGC 3521.

As can be seen from the last row of Table 3, a bright ( $B = 9.8$  mag) neighboring Sbc galaxy NGC 3521 with a radial velocity  $V_h = 737$  km s<sup>-1</sup> is located at a projected separation of 17 deg or 3.0 Mpc from NGC 3115. The radial distances of NGC 3521 (10.7 Mpc) and NGC 3115 (10.2 Mpc) practically coincide with each other within their measurement errors. According to Karachentsev & Kashibadze (2021), NGC 3521 has 6 assumed satellites, of which radial velocities were measured for three. We searched for new dwarf satellites using DECaLS data (Dey et al. 2019). In an area of 4 x 4 degrees (i.e. 750 x 750 kpc), we found four new likely satellites of low surface brightness. Reproductions of their images from DECaLS survey 2' x 2' in size are shown in Fig.5.

A general summary of data on 11 members of the NGC 3521 group is presented in Table 4, the structure of which is similar to that of Table 3. To date, none of the proposed satellites of NGC 3521 have had distances estimated. The average projected separation of the satellites,  $\langle R_p \rangle = 160 \pm 38$  kpc, and their rms velocity relative to NGC 3521,  $\langle \Delta V^2 \rangle^{1/2} = 55$  km s<sup>-1</sup>, turn out to be significantly less than that of the NGC 3115 satellites. The average estimate of the total mass  $M_T = (0.90 \pm 0.42)10^{12}M_{\odot}$  and the ratio  $M_T/L_K = (7 \pm 3)M_{\odot}/L_{\odot}$  indicate a shallow potential well of this galaxy. The rotation curve of NGC 3521, which decreases with distance at periphery (Casertano & van Gorkom 1991), also indicates a low mass of the dark halo of this spiral galaxy.

According to Tully (2015), the virial mass  $M_T$  and virial radius of a group of galaxies  $R_{vir}$  are connected by the empirical relation

$$(R_{vir}/215 \text{ kpc}) = (M_T/10^{12}M_{\odot})^{1/3}.$$

Applying it to the orbital mass estimates of NGC 3115 and NGC 3521, we obtain for them the expected virial radii of 365 kpc with a 1- $\sigma$  confidence interval of [324 – 398] kpc and 208 kpc with a 1- $\sigma$  interval of [168 – 232] kpc, respectively. These values are in good agreement with the average

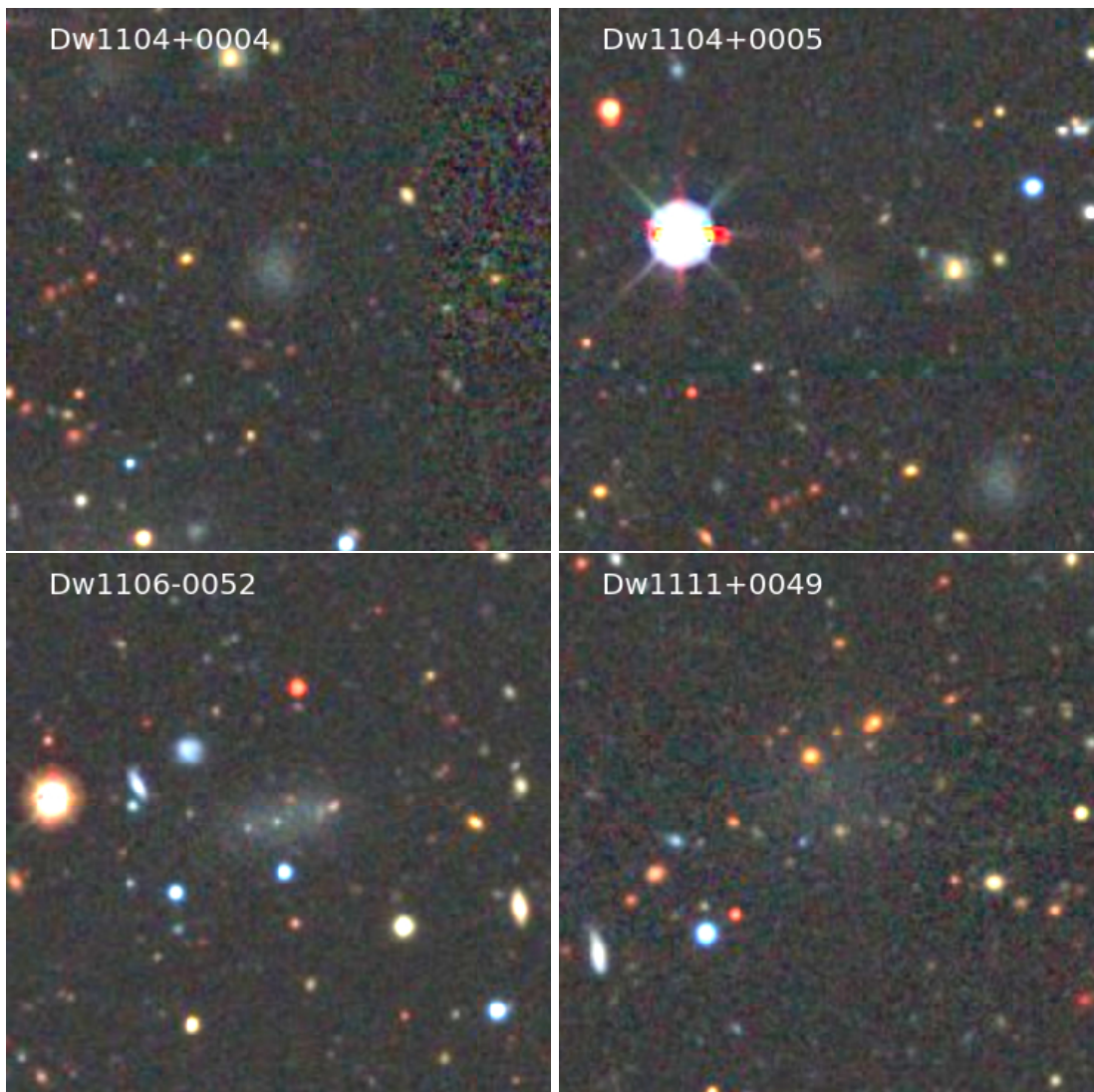


**Figure 5.** Color-composed images of four new probable companions of NGC 3521 taken from DECaLS survey. The size of the images is 2 arcminutes. North is up and east is left.

spatial separation of their satellites,  $\langle R \rangle = (4/\pi)\langle R_p \rangle$ , which is  $(385 \pm 68)$  kpc for NGC 3115 and  $(204 \pm 48)$  kpc for NGC 3521. Therefore, the average size of the suite of satellites around their central galaxy is a good indicator of the virial radius and the dark halo mass of the group. Following the relation by Tully (2015), a significant difference in the observed sizes of suites of these galaxies,  $\langle R_p \rangle_{\text{N3115}} / \langle R_p \rangle_{\text{N3521}} \sim 1.9$ , corresponds to the ratio of their virial mass  $\sim 6$ , which is close to the obtained ratio of the virial masses of these groups,  $\sim 5.4$ . Note that the luminosities of the two parent galaxies are nearly the same: 10.99 dex vs. 11.09 dex.



Both these groups, together with the group around NGC 2784 ( $D = 9.82$  Mpc), are likely part of a diffuse elongated structure "Leo Spur" and "Antlia cloud" (Tully, 1988), that is located near the rich Leo-I galaxy group having  $D = 11.3$  Mpc.

## 5. ISOLATED LUMINOUS EARLY-TYPE GALAXIES IN THE LOCAL VOLUME.

As noted above, in the Local Volume, limited by the distance  $D < 11$  Mpc, there are 5 relatively isolated ETG galaxies with  $L_K/L_\odot$  luminosities brighter than 10.5 dex. Here we do not take into account several bright E and S0 galaxies in the central part of the Leo-I group (NGC 3379, NGC 3384, NGC 3489), which looks like a small cluster with a united dark halo. Data on the 5 detached ETG galaxies are presented in Table 5. The table columns contain: (1) galaxy name; (2) morphological type; (3,4) distance to the galaxy ( Mpc) and the method used to determine the distance; (5) number of known supposed satellites; (6) number of satellites with measured radial velocities; (7) number of satellites with accurate distances measured via TRGB method; (8)  $L_K$  luminosity of ETG galaxy in the  $L_\odot$  units; (9) the ratio of the total (orbital) mass-to- $L_K$ -luminosity in units of  $M_\odot/L_\odot$  according to Karachentsev & Kashibadze (2021).

As one can see, the nearest group around NGC 5128 (Cen A) has been studied in much more detail than the other groups on the outskirts of the Local Volume. The number of assumed satellites around NGC 4594 (Sombrero), NGC 3115, NGC 2784 and NGC 1291 is quite representative (  $n = 17 - 28$ ), but only a small part of them have individual distance estimates and measured radial velocities. The least reliable data are for galaxies in the vicinity of NGC 2784. Five putative satellites of this galaxy: DDO 56, HIPASSJ0916-23b, ESO 497-004, NGC 2835 and DDO 62 are located at projected separations of  $R_p = (220 - 460)$  kpc and they all have a positive difference in radial velocities with respect to NGC 2784. Therefore, the orbital estimate of the mass of this group is highly doubtful. For the other four ETG galaxies, the average ratio of total mass-to-luminosity is  $\langle M_T/L_K \rangle = 58 \pm 6 (M_\odot/L_\odot)$ . Taking, according to Lelli et al. (2016) the value  $M_*/L_K = 0.7 M_\odot/L_\odot$  for the bulge population, we obtain for luminous ETG galaxies the ratio  $\langle M_T/M_* \rangle = 83 \pm 9$ .

## 6. CONCLUDING REMARKS.

**Table 3.** Neighborhood of the galaxy NGC 3115.

Name	RA(2000) ° °	DEC °	T	$D$ Mpc	meth	$V_{LG}$ $\text{km s}^{-1}$	$\log L_K$ $L_\odot$	$r_p$ °	$R_p$ kpc	$\Delta V$ $\text{km s}^{-1}$	$M_{orb}$ $10^{12}$
(1)	(2)	(3)	(4)	(5)	(6)	(7)	(8)	(9)	(10)	(11)	
NGC 3115	151.31	-07.72	-1	10.2	TRGB,a)	439	10.99	0.00	0	0	0.00
KDG 65	151.40	-07.75	-3	10.2	mem	479	8.43	0.09	16	40	0.03
KKSG 18	151.42	-07.98	-1	10.2	mem	456	9.31	0.28	50	17	0.02
dw1006-0730	151.55	-07.50	-2	10.2	mem	—	6.96	0.33	59	—	—
dw1004-0737	150.99	-07.64	-2	7.8	SBF,b)	—	6.57	0.33	59	—	—
dw1006-0732	151.61	-07.55	-2	10.2	mem	—	6.53	0.34	61	—	—
dw1006-0730-n2	151.64	-07.51	10	10.2	mem	—	6.41	0.39	69	—	—
dw1007-0715	151.83	-07.26	-2	10.2	mem	—	7.25	0.69	123	—	—
dw1004-0657	151.16	-06.96	-2	8.8	SBF,b)	—	6.63	0.77	137	—	—
Dw1006-0828	151.65	-08.47	10	10.2	mem	—	5.74	0.82	147	—	—
Dw1007-0835	151.81	-08.59	10	10.2	mem	—	6.17	1.00	178	—	—
dw1007-0830	151.95	-08.50	-2	10.3	SBF,b)	—	6.12	1.01	180	—	—
<i>KKSG 17</i>	150.41	-08.25	10	9.95	TRGB,c)	203	7.87	1.04	185	-236	12.16
dw1002-0642	150.66	-06.71	-2	10.2	mem	—	5.66	1.20	214	—	—
dw1000-0741	150.00	-07.69	10	10.2	mem	—	7.30	1.31	233	—	—
dw1000-0831	150.23	-08.53	-2	10.2	mem	—	6.06	1.35	240	—	—
dw1000-0821	150.04	-08.36	9	10.2	mem	—	7.91	1.42	253	—	—
MCG-01-26-009	150.39	-06.53	10	10.2	mem	510	7.87	1.50	267	71	1.59
<i>UGCA 193</i>	150.65	-06.01	7	10.00	TRGB,c)	427	8.51	1.83	326	-12	0.05
Dw0958-0834	149.52	-08.58	-2	10.2	mem	—	7.09	1.99	354	—	—
KKSG 16	149.94	-09.35	-3	10.2	mem	—	7.89	2.13	379	—	—
Dw0958-0610	149.65	-06.17	-2	10.2	mem	—	7.13	2.27	404	—	—
<i>PGC 154449</i>	149.29	-09.26	9	10.13	TRGB,c)	295	7.92	2.54	452	-144	11.06
LV J0956-0929	149.16	-09.49	9	9.38	TRGB,d)	378	7.95	2.78	495	-61	2.17
KKSG 15	148.79	-06.27	10	10.2	mem	554	8.28	2.91	518	115	8.08
Dw0956-0523	149.23	-05.39	-2	10.2	mem	—	7.21	3.12	556	—	—
<i>PGC 1099440</i>	152.38	-02.18	9	10.39	TRGB,c)	519	8.03	5.64	1004	80	7.58
<i>KKSG 19</i>	156.12	-12.43	10	10.84	TRGB,c)	373	7.70	6.73	1198	-66	6.16
AGC 202137	155.41	+00.90	10	8.59	NAM	495	7.21	9.55	1700	56	6.29
PGC 4078844	143.84	-13.81	9	9.06	TF,e)	533	7.60	9.64	1716	94	17.89
UGC 5797	159.85	+01.72	9	10.42	TRGB,d)	511	8.63	12.73	2266	72	13.86
NGC 3521	166.45	-00.04	4	10.70	TF,e)	598	11.09	16.98	3022	159	(90.15)

Notes: a) Peacock et al.2015; b) Carlsten, personal communication; c) present paper;

d) Anand et al. 2021; e) Karachentsev et al. 2013.

Alternative names: KDG 65 = UGCA 200 = PGC 29299, KKSG 18 = MCG-01-26-021 = PGC 29300, KKSG 17 = MCG-01-26-011 = PGC 29033, MCG-01-26-009 = PGC 29038, UGCA 193 = PGC 29086, KKSG 16 = PGC 3097699, PGC 154449 = 2MASX J09570887-0915487, LV J0956-0929 = PGC 4078671, KKSG 15 = PGC 1034827, PGC 1099440 = 2dFGRS-TGN218Z179, KKSG 19 = HIPASS J1024-12 = PGC 3097700.

**Table 4.** Probable satellites of the galaxy NGC 3521.

Name	RA(2000)DEC °	T	$D$ Mpc	meth	$V_{LG}$ km s <sup>-1</sup>	$\log L_K$ $L_\odot$	$r_p$ °	$R_p$ kpc	$\Delta V$ km s <sup>-1</sup>	$M_{orb}$ 10 <sup>12</sup>
(1)	(2)	(3)	(4)	(5)	(6)	(7)	(8)	(9)	(10)	(11)
NGC 3521	166.45−00.04	4	10.7	TF	598	11.09	0	0	0	0
N3521sat	166.42 +00.12	−1	10.7	mem	−	8.62	0.16	30	−	−
KKSG 20	166.17 +00.06	10	10.7	mem	636	7.63	0.30	56	38	0.10
Dw1104+0005	166.17 +00.09	−2	10.7	mem	−	6.58	0.31	58	−	−
Dw1104+0004	166.16 +00.08	−2	10.7	mem	−	7.02	0.32	59	−	−
N3521dwTBG	166.80−00.19	−2	10.7	mem	−	7.28	0.38	72	−	−
Dw1106-0052	166.61−00.88	10	10.7	mem	−	6.67	0.86	161	−	−
dw1110+0037	167.62 +00.62	10	10.7	mem	669	7.62	1.34	252	71	1.50
KKSG 22	166.53−01.45	10	10.7	mem	−	7.11	1.41	265	−	−
Dw1111+0049	167.85 +00.83	10	10.7	mem	−	6.67	1.64	306	−	−
UGC 6145	166.39−01.86	10	10.7	mem	546	7.83	1.82	341	−52	1.09

Alternative names: KKSG 20 = PGC 135770, dw1110+0037 = SDSS J111029.56+003700.7.

**Table 5.** Isolated early-type galaxies in the Local Volume with  $L_K/L_\odot > 10.5$  dex.

(1)	(2)	(3)	(4)	(5)	(6)	(7)	(8)	(9)
Name	Type	$D$	meth	$n$	$n_v$	$n_{TRGB}$	$\log(L_K)$	$M_T/L_K$
NGC 5128	S0p	3.68	TRGB	62	34	43	10.89	60±18
NGC 4594	S0a	9.55	TRGB	27	15	3	11.32	74±24
NGC 3115	S0	10.2	TRGB	27	10	6	10.99	50±15
NGC 2784	S0	9.82	SBF	28	5:	0	10.80	145±50:
NGC 1291	SB0a	10.97	TRGB	17	2	1	10.97	47±4

Relatively isolated E,S0 galaxies in the Local Volume with luminosity of  $\log(L_K/L_\odot) > 10.5$  have the average luminosity of  $\langle \log(L_K/L_\odot) \rangle = 10.99 \pm 0.09$  and the average total mass-to-luminosity ratio  $\langle M_T/L_K \rangle = 58 \pm 6 (M_\odot/L_\odot)$ . There are only 5 such galaxies out of 1200 galaxies in the Local Volume. Despite the poor statistics, these parameters turn out to be quite representative for the population of massive ETG galaxies. Thus, a sample of 26 isolated E,S0 galaxies of the northern sky from the KIG-catalog, which have faint companions with measured radial velocities, is characterized by the values:  $\langle \log(L_K/L_\odot) \rangle = 11.01 \pm 0.06$  and  $\langle M_T/L_K \rangle = 74 \pm 26 (M_\odot/L_\odot)$  (Karachentseva et al. 2021a). For 60 isolated ETG galaxies from the 2MIG catalog, in which the radial velocities of satellites were measured, the median parameters are  $\log(L_K/L_\odot) = 11.13$  and  $M_T/L_K = 63 (M_\odot/L_\odot)$

(Karachentseva et al. 2011). Note that both catalogs of isolated galaxies, KIG and 2MIG, selected from optical and infrared (2MASS) sky surveys, cover significant volume up to redshift  $z \sim 0.02$ .

A similar analysis of data on 141 dwarfs with known radial velocities around isolated spiral KIG-galaxies gives an average ratio of  $\langle M_T/L_K \rangle = 20.9 \pm 3.1(M_\odot/L_\odot)$  (Karachentseva et al. 2021b). For isolated spiral galaxies of the 2MIG catalog, the median of this ratio via 154 satellites is  $17 M_\odot/L_\odot$  (Karachentseva et al. 2011). Part of this difference is obviously due to different  $M_*/L_K$  ratios for the stellar population of the disk ( $0.5 M_\odot/L_\odot$ ) and bulge ( $0.7 M_\odot/L_\odot$ ) (Lelli et al. 2016). Generally, the available data on the motions of faint satellites around isolated high-luminosity galaxies definitely indicate a (2–3)-fold excess of dark matter around bulge-dominated galaxies compared to disk-dominated ones of the same stellar mass. This conclusion is consistent with the assertions: ”we find that passive central galaxies have halos that are at least twice massive as those of star-forming objects of the same stellar mass” (Mandelbaum et al. 2016) and ”the red galaxies occupy dark matter halos that are much more massive than those occupied by blue galaxies with the same stellar mass” (Bilicki et al. 2021), both obtained from the weak gravitational lensing data.

Despite the limited statistics, there is also a noticeable tendency according to which the variation in the ratio of dark-to-light matter ( $M_T/M_*$ ) in late-type galaxies is much wider than in early-type galaxies. Moreover, some spiral galaxies with a decreasing rotation curve at the periphery (NGC 253, NGC 2683, NGC 2903, NGC 3521 and NGC 5055) have an anomalously low ratio  $M_T/L_K \sim 5M_\odot/L_\odot$  (Karachentsev et al. 2021). The observed diversity of luminous galaxies of different morphological types in terms of the  $M_T/L_K$  parameter has not yet found a clear theoretical interpretation.

We are grateful to the anonymous referee for a prompt report that helped us improve the manuscript. This work is based on observations made with the NASA/ESA Hubble Space Telescope. Support for program SNAP–15922 (PI R.B.Tully) was provided by NASA through a grant from the Space Telescope Science Institute, which operated by the Associations of Universities for Research in Astronomy, Incorporated, under NASA contract NASb5-26555. Part of the work was made using the facilities of the Big Telescope Alt-azimutal SAO RAS and supported under the Ministry of Science and Higher Education of the Russian Federation grant 075-15-2022-233 (13.MNPMU.21.0003).

We used also data obtained with the Dark Energy Camera Legacy Survey (DECaLS) founded by the U.S. Department of Energy, the U.S. National Science Foundation.

## References

- Anand G.S., Rizzi L., Tully R.B., et al., 2021, *AJ*, 162, 80
- Bilek M., Samurovic S., Renauld F., 2019, *A & A*, 629L, 5
- Bilicki M., Dvornik A., Hoekstra H., et al. 2021, *A & A*, 653A, 82
- Capaccioli M., Cappellaro E., Held E.V., Vierti M., 1993, *A & A*, 274, 69
- Carlsten S.G., Greene J.E., Greco J.P., et al. 2021a, *ApJ*, 922, 267
- Carlsten S.G., Greene J.E., Beaton R.L., Greco J.P., 2021b, arXiv:2105.03440
- Casertano S. & van Gorkom J.H., 1991, *AJ*, 101, 1231
- Colles M., Peterson B.A., Jackson C.A. et al. 2003, arXiv:astro-ph/0306581 (2dF)
- Dey A., Schlegel D.J., Lang D., et al. 2019, *AJ*, 157, 168
- Dolphin, A.E. 2000, *PASP*, 112, 1383
- Dolphin, A.E. 2016, DOLPHOT: Stellar photometry, ascl:1608.013
- Doyle M.T., Drinkwater M.J., Rohde D.J. et al. 2005, *MNRAS*, 361, 34
- Guerou A., Emsellem E., Krajnovich D., et al. 2016, *A & A*, 591A, 143
- Huchtmeier W.K., Karachentsev I.D., Karachentseva V.E., 2001, *A & A*, 377, 801
- Ibata R.A., Ibata N.G., Lewis G.F., et al, 2014, *ApJ*, 784L, 6
- Jones D.H., Read M.A., Saunders W., et al. 2009, *MNRAS*, 399, 683 (6dF)



- Karachentsev I.D., Kashibadze O.G., 2021, AN, 342, 999
- Karachentsev I.D., Tully R.B., Anand G.S., et al. 2021, AJ, 161, 205.
- Karachentsev I.D., Makarova L.N., Tully R.B., et al. 2020, A & A, 643A, 124
- Karachentsev I.D., Kudrya Y.N., 2014, AJ, 148, 50
- Karachentsev I.D., Makarov D.I., Kaisina E.I., 2013, AJ, 145, 101
- Karachentsev I.D., Karachentseva V.E., Suchkov A.A., Grebel E.K., 2000, A & AS, 145, 41
- Karachentseva V.E., Karachentsev I.D., Melnyk O.V., 2011, Astrophys. Bull., 66, 389
- Karachentseva V.E., Karachentsev I.D., Melnyk O.V., 2021a, Astrophys. Bull., 76, 124
- Karachentseva V.E., Karachentsev I.D., Melnyk O.V., 2021b, Astrophys. Bull., 76, 341
- Kourkchi E., Tully R.B., 2017, ApJ, 843, 16
- Lapi A., Salucci P., Danese L., 2018, ApJ, 859, 2
- Lelli F., McGaugh S.S., Schombert J.M., 2016, AJ, 152, 157
- Libeskind N.I., Hoffman Y., Tully R.B., et al. 2015, MNRAS, 452, 1052
- Makarov, D.I., Prugniel P., Terekhova N., et al, 2014, A&A, 570A, 13
- Makarov, D.I., Makarova, L.N., Rizzi, L. et al., 2006, AJ, 132, 2729
- Mandelbaum R., Wang W., Zu Y., et al, 2016, MNRAS, 457, 3200
- Mateo M., 1998, ARA & A, 36, 435
- Moster B.P., Naab T., White S.D.M., 2013, MNRAS, 428, 3121
- Muller O., Pawlowski M.S., Jerjen H., Lelli F., 2018, Sci, 359, 534
- Pawlowski M.S., Kroupa P., Jerjen H., 2013, MNRAS, 435, 2116
- Peacock M.B., Strader J., Romanowsky A.J., Brodie J.P., 2015, ApJ, 800, 13
- Peng E.W., Ford H.C., Freeman K.C., 2004, ApJ, 602, 685
- Posti L. & Fall S.M., 2021, A & A, 649, 119
- Rizzi, L., Tully, R.B., Makarov, D.I. et al. 2007, ApJ, 661, 815
- Sales L.V., Wang W., White S.D.M., Navarro J.F., 2013, MNRAS, 428, 573
- Santos-Santos I.M.E., Sales L.V., Fattahi A., Navarro J.F., 2021, arXiv:2111.01158
- Schlafly, E.F., Finkbeiner, D.P. 2011, ApJ, 737, 103

- Shaya E.J., Tully R.B., Hoffman Y., et al, 2017, ApJ, 850, 207
- Tonry J.L., Dressler A., Blakeslee J.P., et al. 2001, ApJ, 546, 681
- Tully R.B., 2015, AJ, 149, 54
- Tully R.B., 1988, Nearby Galaxies Catalog, Cambridge University Press, Cambridge
- Vorontsov-Veliaminov B.A., Arkhipova V.P., 1963, Morphological Catalog of Galaxies, part III, Moscow State University, Moscow
- Wechsler R.H. & Tinker L.J., 2018, ARA&A, 56, 435
- Wegner G., Bernardi M., Willmer C.N.A., et al. 2003, AJ, 126, 2268
- Wu, P.-F., Tully, R.B., Rizzi, L. et al. 2014, AJ, 148, 7